BMC Genomics

RESEARCH

Open Access

Comparative transcriptomic and metabolomics analysis of ovary in *Nilaparvata lugens* after trehalase inhibition

Yongkang Liu[1†], Fan Yang[1†], Sijing Wan[1], Xianzhong Wang[1], Liwen Guan[1], Yan Li[1], Caidi Xu[2], Binghua Xie[1], Shigui Wang[1], Xiao-Ling Tan[3,4*] and Bin Tang[1*]

Abstract

The fecundity of *Nilaparvata lugens* (brown planthopper) is influenced by trehalase (TRE). To investigate the mechanism by which trehalose affects the reproduction of *N. lugens*, we conducted a comparative transcriptomic and metabolomic analysis of the ovaries of *N. lugens* following injection with dsTREs and validamycin (a TRE inhibitor). The results revealed that 844 differentially expressed genes (DEGs) were identified between the dsGFP and dsTREs injection groups, with 317 up-regulated genes and 527 down-regulated genes. Additionally, 1451 DEGs were identified between the water and validamycin injection groups, with 637 up-regulated genes and 814 down-regulated genes. The total number of DEGs identified between the two comparison groups was 236. The overlapping DEGs were implicated in various biological processes, including protein metabolism, fatty acid metabolism, AMPK signaling, mTOR signaling, insulin/insulin-like growth factor signaling (IIS), the tricarboxylic acid (TCA) cycle, oxidative phosphorylation, and the cellular process of meiosis in oocytes. These results suggest that the inhibition of *TRE* expression may lead to alterations in ovarian nutrient and energy metabolism by modulating glucose transport and affecting amino acid metabolic pathways. These alterations may influence the reproduction of *N. lugens* by modulating reproductive regulatory signals. These findings provide robust evidence supporting the mechanism through which trehalase inhibition reduces the reproductive capacity of *N. lugens*.

Keywords *Nilaparvata lugens*, Transcriptomic, Metabolomics, Ovary development, Trehalase

Introduction

Nilaparvata lugens, commonly known as the brown planthopper, is a notorious pest in paddy fields that feeds on the rice phloem and damages rice tissues [1]. *N. lugens* is also a vector of rice viruses, which facilitates the spread of the virus and contributes to significant losses in global rice production [2, 3]. The primary strategy to manage the *N. lugens* population relies on the application of chemical insecticides [4]. However, the extensive use of chemical pesticides has resulted in insecticides resistance of *N. lugens*, including physiological resistance and target mutations [5–7]. Consequently, there is an urgent need to develop environmentally friendly and effective

†Yongkang Liu and Fan Yang contributed equally to this work.

*Correspondence:
Xiao-Ling Tan
tanxiaoling@caas.cn
Bin Tang
tbzm611@hznu.edu.cn
[1]College of Life and Environmental Sciences, Hangzhou Normal University, Hangzhou, Zhejiang 311121, P.R. China
[2]Chinese Education Modernization Research Institute of Hangzhou Normal University, Hangzhou Normal University, Hangzhou, Zhejiang 311121, P.R. China
[3]State Key Laboratory for Biology of Plant Diseases and Insect Pests, Institute of Plant Protection, Chinese Academy of Agricultural Sciences, Beijing 100193, P.R. China
[4]Zhongyuan Research Center, Chinese Academy of Agricultural Sciences, Xinxiang 453500, P.R. China

alternatives, such as RNA biopesticides [8–12], as well as other environmentally sustainable compounds to safely control pests [13, 14]. Trehalose is the primary circulating sugar during the development of insect oocytes [15, 16]. Trehalase serves as the rate-limiting enzyme in trehalose degradation, and its inhibition directly impedes the trehalose hydrolysis [17]. Currently, two distinct forms of trehalase, soluble trehalase (TRE1) and membrane-bound trehalase (TRE2), have been identified in various insect such as *N. lugens*, *Tribolium castaneum*, *Tenebrio molitor*, *Bombyx mori*, and *Apis mellifera* [18–20]. As a key enzyme in trehalose metabolism, multiple *TRE1* genes have been identified in insects such as *N. lugens*, *Harmonia axyridis*, and *Tribolium castaneum*, with two isoforms, *TRE1-1* and *TRE1-2*, observed in *N. lugens* [19–21]. Furthermore, previous studies have shown that both *TRE1* and *TRE2* regulate larval development, molting as well as pupation in insects, through the chitin pathway [24]. Therefore, the development of trehalase inhibitors represents a promising approach for exploiting pesticides [23–25]. To date, several natural trehalase inhibitors have been found, including validamycin, salbostatin, trehazolin, natural iminosugars, and thiazolidinone compounds [30–33].

The reproductive control network of insects is complex. The insulin/insulin-like peptide signaling pathway (IIS) is a highly conserved signaling cascade [22]. IIS is initiated by insulin-like peptides (ILPs), which bind to the insulin receptor (InR), a transmembrane receptor on the cell surface. This binding induces autophosphorylation of InR and the recruitment of the insulin receptor substrate Chico, which is subsequently also phosphorylated. This process activates phosphoinositide 3-kinase (PI3K), which then phosphatidylinositol 4,5-diphosphate (PIP2) to produce phosphatidylinositol 3,4,5-trisphosphate (PIP3). PIP3, in turn, activates protein kinase B (Akt), which further regulate the gene expression such as Forkhead box O (Foxo) [26]. Studies in *N. lugens* have demonstrated that the transcription factor Foxo directly regulates the expression of vitellogenin (Vg) by acting on its exon [27]. Currently, two TOR complexes, termed TORC1 and TORC2, have been identified. However, it is widely accepted that only TORC1 is responsive to rapamycin, positioning TORC1 as the central complex in the TOR signaling pathway [28]. As a nutrient sensor, the Target of rapamycin (TOR) signaling pathway regulates various physiological processes in response to the nutritional condition. As upstream of the TOR pathway, amino acids (AAs) enter the cytoplasm via amino acid transmembrane receptors, where they bind to intracellular RAS-related small GTPases or Rags, thereby activating the TOR pathway [27–29]. Finally, the phosphorylation of S6 kinase (S6K) and 4E-binding protein 1 (4E-BP1) arise as the downstream events [28]. Phosphorylated S6K participates in the transcriptional and translational regulation of *Vg* [34]. Additionally, TOR can stimulate the secretion of ILPs, thereby activating the IIS pathway, which indirectly influences insect reproduction [29]. The reproductive system of female insects consists of a pair of ovaries, each containing numerous ovarian cells. The number of ovaries varies among insect species, and there are also differences between the left and right ovaries within the same individual [35, 36]. Previous studies have shown that feeding glucose can enhance the reproductive efficiency of bees, as carbohydrate supplements provide the energy necessary for egg maturation [37]. TRE activity has been detected in ovaries containing oocytes, suggesting that TRE plays a crucial role in ovarian development [38, 52]. Moreover, ovarian development and fecundity in *N. lugens* were reduced after TRE inhibition (unpublished). However, the underlying mechanism remains unknown.

Omics is a comprehensive approach that investigates the functions, relationships, and interactions of various molecules within organisms [39], encompassing fields such as transcriptomics, metabolomics, and proteomics, among others [39–40, 42–43]. Among them, RNA sequencing (RNA-seq) is an important method that performs transcriptome analysis using deep sequencing technology [43–45]. To comprehensively investigate the molecular mechanisms or interactions underlying the effects of different treatments on organisms, RNA-seq is the most effective method for identifying differentially expressed genes (DEGs) [46, 47]. Metabolomic sequencing, emerging as a biological research tool alongside RNA-seq, is utilized to quantify metabolic changes through gene interference or diverse condition treatments, thereby establishing a link between gene expression and phenotype. Therefore, metabolomics sequencing can establish a link between gene expression and phenotype [48]. By comparing and analyzing the results of transcriptomic and metabolomic sequencing, a more comprehensive understanding of the molecular mechanisms underlying these changes can be obtained. This approach has also been applied across various organisms [49, 50]. In this study, comparative transcriptomic and metabolomic analyses were conducted on the ovaries of female *N. lugens* after TRE inhibition, and the potential molecular mechanisms by which TRE regulates reproduction in *N. lugens* were investigated.

Materials and methods

Insect rearing

Taichung Native 1 (TN1) was used to feeding *N. lugens*, which were collected from the field area of the China National Rice Research Institute. The environmental conditions in the artificial climate chamber were maintained

as follows: temperature 27 ± 1 °C, relative humidity 65 ± 5%, and photoperiod of 18 L : 6D (Light: Dark).

dsRNA synthesis and microinjection

Five adults were added to Trizol (Takara, Japan) and homogenized with steel beads. RNA was subsequently separated and precipitated using chloroform and isopropanol, followed by being washed with 75% ethanol and resuspended with RNase-free water. The cDNA was synthesized using the PrimeScript^{TM} RT Reagent Kit with gDNA Eraser (Takara, Japan), following the manufacturer instructions. PCR amplification was carried out using primers (Table 1) synthesized by SunYa (Zhejiang, China). dsRNA synthesis was performed according to the T7 RiboMAX Express RNAi System (Promega, Madison, USA). A green fluorescent protein (GFP) gene amplicon was used as a control. Newly emerged female long-winged adults of *N. lugens* were selected and injected using a TransferMan 4r microinjector (Eppendorf, Hamburg, Germany). In this study, four injection groups were set up: (1) dsGFP; (2) the synthesized dsTRE1-1, dsTRE1-2 and dsTRE2 were mixed into dsTREs according to 1: 1: 1; (3) double distilled water ddH_2O, marked as ddWater; (4) Validamycin (Dr. Ehrenxtorfer, Germany). The concentration of dsRNA for injection was 4000 ng/μL, and the concentration of validamycin for injection was 0.5 μg/μL. Each individual was injected with 100 nL solution [53,54].

Sampling for transcriptomic and metabolomics sequencing

The injected female and untreated male were paired in a 1:1 ratio and reared for 3 days, and the ovaries of females were collected. Three biological replicates were performed, with each replicate consisting of 5–10 ovaries. Total RNA from ovaries was extracted for transcriptome sequencing performed by Beijing Genomics Institute (Shenzhen, China). Subsequently, mRNA library was constructed and sequenced by DNBSEQ sequencing platform to obtain the raw data. Similarly, six biological replicates were collected for non-targeted metabolomics sequencing performed by Beijing Genomics Institute (Shenzhen, China), with each replicate containing 15–25 ovaries.

Transcriptome data analysis

The raw reads were filtered using SOAPnuke software to obtain clean reads. HISAT was used to align clean reads to the reference genome of *N.lugens* (GCF 014356525.1) for new transcript prediction, SNP analysis, InDel analysis, and differential splicing gene detection [60]. The sequences with protein-coding potential in the obtained new transcripts were added to the reference gene sequence to form a complete reference sequence, and the expression level was calculated using RSEM [61]. The DEGs were screened using DEseq2. All DEGs were annotated using NR databases, followed by GO functional annotation with Blast2GO software (v2.5.0). The differentially expressed genes were classified into functional categories based on GO annotation. Enrichment analysis was performed using the phyper function in R software, and q-value ≤ 0.05 was considered significantly enriched [62].

RT-qPCR verification

Five to six *N. lugens* individuals were injected and collected for RNA extraction and cDNA synthesis, with each treatment group repeated 3–4 times. Primers were designed and synthesized (Table 2). The synthesized cDNA was used as a template for RT-qPCR, with the *actin* gene acting as the internal reference. RT-qPCR was performed using a real-time PCR detection system (Bio-Rad, Hercules, USA). Genes involved in glucose metabolism, lipid metabolism, chitin metabolism as well as reproductive regulation were selected for RT-qPCR validation, with nine genes between the dsGFP and dsTREs groups, and twelve genes between the water and validamycin groups. Gene IDs for the validation genes are provided in Table 3, and the primers used for quantification are listed in Table 2.

Metabolite extraction and LC-MS/MS analysis

An extraction solution was prepared by mixing methanol, acetonitrile, and water. A 25 mg sample of *N. lugens*

Table 1 Primers for dsRNA synthesis

Primer name	Forward primer (5′-3′)	Reverse primer (5′-3′)
NITRE1-1	GATGCAATCAAGGAGGTGTTATGGC	CGTATTCACCTCCACCTCCGT
NITRE1-1-T7	T7-GATGCAATCAAGGAGGTGTTATGGC	T7-CGTATTCACCTCCACCTCCGT
NITRE1-2	AGATGAAGGCATGTGGTTCG	CATCGATTCGCCAACTGGTAAGC
NITRE1-2-T7	T7-AGATGAAGGCATGTGGTTCG	T7-CATCGATTCGCCAACTGGTAAGC
NITRE2	CCAACTGCTATGACACCGACAAG	GGGTTCAGATCCTGCCGTCGCT
NITRE2-T7	T7-CCAACTGCTATGACACCGACAAG	T7-GGGTTCAGATCCTGCCGTCGCT
GFP	AAGGGCGAGGAGCTGTTCACCG	CAGCAGGACCATGTGATCGCGC
GFP-T7	T7-AAGGGCGAGGAGCTGTTCACCG	T7-CAGCAGGACCATGTGATCGCGC

T7 sequence:5′- GGATCCTAATACGACTCACTATAGG-3′

Table 2 Primers for RT-qPCR

Gene ID	Forward primer (5′-3′)	Reverse primer (5′-3′)
111,043,495	GAACCTGCAGGCCAAACACA	ACCACTCGGTTGGGCTGAAT
111,043,686	CCCAGGAGAACAAGGTTTAGTG	CAAGGGCTGCCAGACAGTAG
111,045,055	GGACGGTGCTTCTTTTGGA	GTGAGGCATCGGCTCTGTT
111,045,930	CTGATCCGCGAGACCTATGC	GCGATGACCTGTCCTTGCTAC
111,046,157	GGCGTTCATCTGCTGCTTC	GACTTGCGACACTTGTCCACC
111,046,883	ACTCGCCAGCACAGCAAAA	CAGCCTACCAAACCATGAAGAT
111,047,049	GGGTGGGACAAGACTTACTGC	CCCGATGGTCTTTGAATGGA
111,052,579	AGGCAGCCACACAGATAACCGC	AGCCGCTCGCTCCAGAACATT
111,054,583	CGGTTATCCGAAATGTCCAGT	TCTCCATCTTGTAGCCCCAGT
111,046,048	CCGCAAACGATTCCTACAGA	AGGTCCTTGACGCTCATTCC
111,047,475	CTCTTGCCGAACAGCCTTAC	GGGTCGTTTAGTGGGTCTGA
111,049,718	GTCGCCTTCTCCGCTATTCT	CCATGCCGTTTCCTCTTTG
111,052,473	CGGTTCCGATTGTCAGTTTG	TGCTGGTCCCTTGATCTGTG
111,053,657	ATGTCTGATTGTCTTGGGAGGC	CCAAGTGAGAATACCACGATGAAC
111,056,107	GAGTGCAACCCGGAGTATGT	TCTTGACGGCACACTTCTTG
111,056,142	TCACGGTTGTCCAAGTCT	TGTTTCGTTTCGGCTGT
111,059,194	AAGACTGAGGCGAATGGT	AAGGTGGAAATGGAATGTG
111,061,289	CACTGCCCGTGCTGTGCTCTA	TGACTTCCTTGCTTTGCTCCC

Table 3 Annotated information of genes

Gene ID	Control group	q value	Gene prediction
111,043,495	dsGFP VS dsTREs	0.00016489	juvenile hormone acid methyltransferase
111,043,686	dsGFP VS dsTREs	0.003817801	fatty acid elongase
111,045,055	dsGFP VS dsTREs	0.00000328	glucose dehydrogenase -like
111,045,930	dsGFP VS dsTREs	0.012180559	fatty acid synthase
	ddWater VS Validamycin	0.020274116	
111,046,157	dsGFP VS dsTREs	0.028126215	facilitated trehalose transporter Tret1-like
111,046,883	dsGFP VS dsTREs	0.032763938	facilitated trehalose transporter Tret1-like
	ddWater VS Validamycin	0.003144976	
111,047,049	dsGFP VS dsTREs	0.03238005	phosphomannomutase
111,052,579	dsGFP VS dsTREs	0.001192282	vitellogenin receptor
	ddWater VS Validamycin	0.000408648	
111,054,583	dsGFP VS dsTREs	0.000000000000755	glucose dehydrogenase -like
111,046,048	ddWater VS Validamycin	0.046346314	chitin synthase 1 variant a
111,047,475	ddWater VS Validamycin	0.000726376	insulin receptor 2
111,049,718	ddWater VS Validamycin	0.021621264	sugar transporter
111,052,473	ddWater VS Validamycin	0.0000127	sugar transporter 1
111,053,657	ddWater VS Validamycin	0.040343716	sugar transporter 11
111,056,107	ddWater VS Validamycin	0.029915112	insulin receptor 1
111,056,142	ddWater VS Validamycin	0.004094465	membrane-bound trehalase
111,059,194	ddWater VS Validamycin	0.000852713	trehalose 6-phosphate synthase
111,061,289	ddWater VS Validamycin	0.003236295	vitellogenin

ovaries was added to 800 μL of the extraction solution and 10 μL of the internal standard, then pulverized and homogenized. The mixture was subsequently centrifuged, and the supernatant was dried using a freeze-vacuum concentrator. The dried sample was then re-dissolved and centrifugation. The supernatant was transferred for LC-MS analysis. From each sample, 20 μL of supernatant was collected and pooled to form a QC sample, which was analyzed by LC-MS alongside the samples from each treatment group. The extracted metabolites were separated and detected in both positive and negative ion modes using a Q Exactive HF high-resolution mass spectrometer (Thermo Fisher Scientific, USA).

Non-targeted metabolomics analysis

In this experiment, the internal standards for untargeted metabolomics included L-Leucine-d3, L-Phenylalanine (13C9, 99%), L-Tryptophan-d5, and Progesterone-2,3,4-13C3. Data were processed using Compound Discoverer 3.1 software (Thermo Fisher Scientific, USA). The

identified compounds were classified and annotated using the KEGG database and the Human Metabolome Database (https://hmdb.ca/). Functional characteristics, major metabolic pathways, and signaling pathways associated with the identified metabolites were determined through functional annotation with the KEGG database. The overall distribution of individual samples within each group and the dispersion between groups were assessed by principal component analysis (PCA). The variable importance for the projection (VIP) of the first two principal components was calculated using the partial least squares discriminant analysis (PLS-DA) model. Fold change (FC) values were calculated through fold change analysis, and statistical significance was assessed using *t*-tests, with *q*-values corrected using the false discovery rate (FDR). Differential metabolites were screened when VIP ≥ 1, FC ≥ 1.2 or ≤ 0.8, and *q*-value < 0.05. Hierarchical clustering analysis was conducted and metabolic pathway enrichment analysis was performed based on the KEGG database, with *p*-values < 0.05 considered significantly enriched.

Results

DEGs analysis

RNAi treatment significantly reduced the expression of trehalase genes *NlTRE1-1*, *NlTRE1-2*, and *NlTRE2* in adult female *N. lugens*, as confirmed by qRT-PCR analysis (Fig. S1). A total of 844 DEGs were identified between the dsGFP and dsTREs injection groups, with 317 up-regulated and 527 down-regulated genes (Fig. 1A). Similarly, 1451 DEGs were identified between the water and validamycin injection groups, including 637 up-regulated and 814 down-regulated genes (Fig. 1A). The number of DEGs shared between the two control groups was 236 (Fig. 1B).

Go function analysis of DEGs

Three categories, including molecular function (MF), cellular component (CC), and biological process (BP), were classified by GO database. Among the DEGs between the dsGFP and dsTREs groups, 651 genes were associated with MF, 615 with CC, and 564 with BP functions (Fig. S2A). In terms of MF, differential genes were mainly related to binding, catalytic activity, and transport activity. In the CC category, genes were mainly related to cell structure and intracellular processes, while in the BP category, genes involved in intracellular processes, biological regulation, and metabolic processes were the most abundant (Fig. 2A). In the DEGs regulated by validamycin, 1239 genes were associated with MF, 1102 with CC, and 1084 with BP functions (Fig. S2B). Similarly, DEGs were mainly related to binding, catalytic activity, transport activity, and structural molecular activity in MF. In the CC category, DEGs were mainly associated with cell structure and intracellular processes were the most prevalent, while in the BP category, genes involved in intracellular processes, biological regulation, and metabolic regulation were the most abundant (Fig. 2B).

KEGG metabolic pathway analysis of DEGs

Results revealed that the DEGs in the dsTREs group were associated with 221 metabolic pathways, among which the significantly enriched pathways included protein export, fatty acid metabolism, proteasome pathway, endoplasmic reticulum protein processing, cardiac muscle contraction, and fatty acid elongation (Fig. 3A). The DEGs regulated by validamycin were distributed across 237 metabolic pathways, with significant enrichment in ribosome biogenesis, glutathione metabolism, and the longevity-regulating pathway in worms (Fig. 3B). It is noteworthy that DEGs of two group were widely involved in metabolic pathways related to fatty acids, lysine, proline, carbohydrates, and energy metabolism, including the TCA cycle and oxidative phosphorylation. Furthermore, signal transduction pathways associated with reproduction and energy regulation, such as AMP-activated protein kinase pathway (AMPK), mammalian target of rapamycin pathway (mTOR), and IIS signaling pathways, were also enriched with DEGs, and the cellular process of oocyte meiosis was similarly affected (Fig. 3C). Overall, these results have suggested that TRE inhibition may impair oxidative phosphorylation and the TCA cycle by altering the nutrients and energy metabolism, ultimately disrupting the reproductive regulatory network.

Validation of DEGs

There were 9 DEGs and 12 DEGs were selected for validation after dsTREs or validamycin injection, respectively. Results showed that their relative expression trends were consistent with those observed in the transcriptome data, indicating the reliability of the transcriptome sequencing (Fig. 4).

Statistics of differential metabolites

A total of 129 differential metabolites were identified and screened between the dsGFP and dsTREs groups in negative ion mode, of which 88 metabolites were up-regulated and 41 metabolites were down-regulated (Fig. 5A). In positive ion mode, a total of 439 differential metabolites were identified between the dsGFP and dsTREs groups, with 296 metabolites up-regulated and 143 metabolites down-regulated (Fig. 5B). For the validamycin-treated group, a total of 154 differential metabolites were screened in negative ion mode compared with the control group, of which 58 metabolites were up-regulated and 96 metabolites were down-regulated (Fig. 5C). Similarly, 457 metabolites were screened in positive ion mode, of which

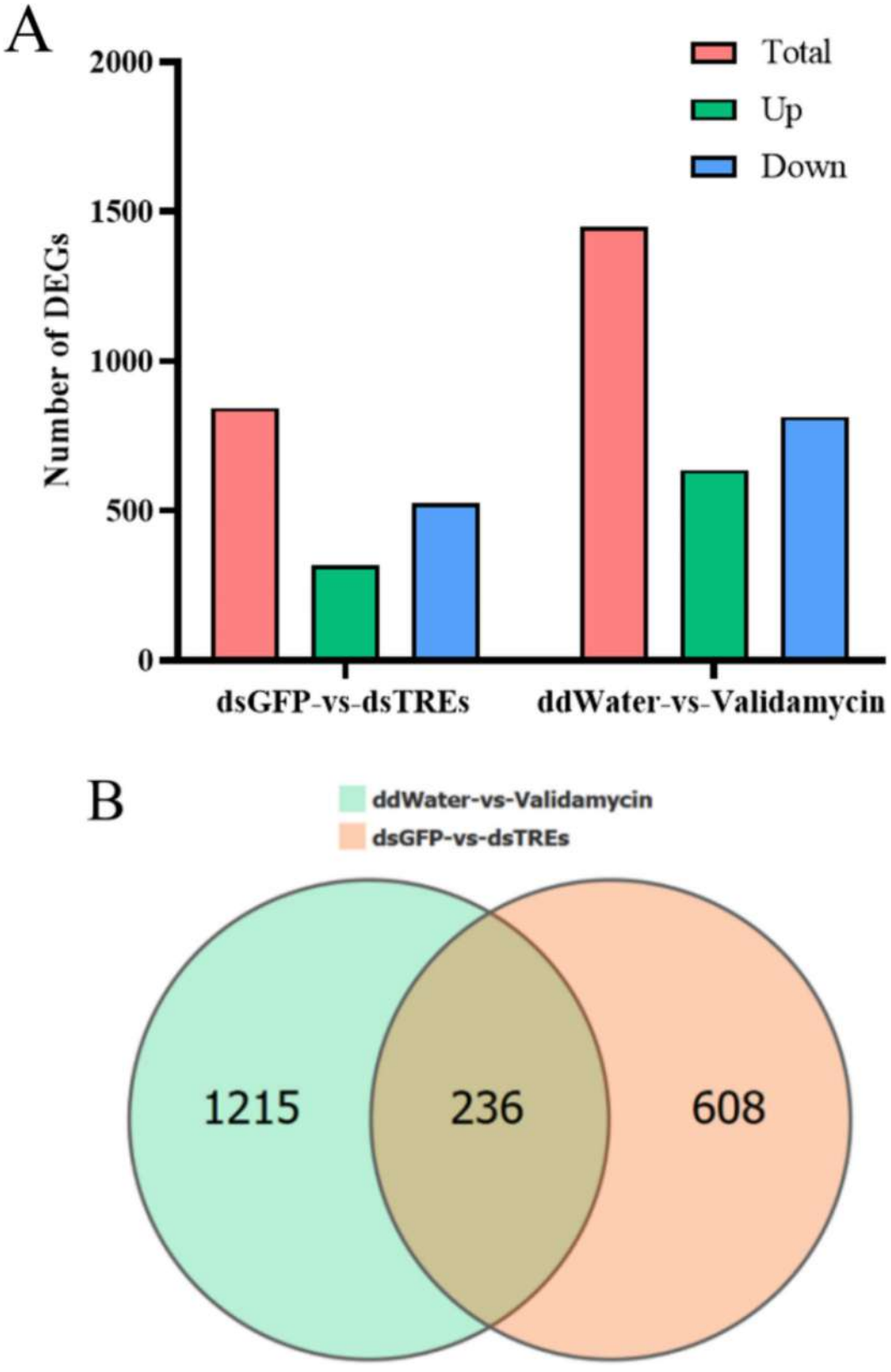

Fig. 1 The number of DEGs between groups. The number of up-regulated and down-regulated genes (**A**) and differentially expressed genes between different comparison groups (**B**) after dsTREs and validamycin injection. Three biological replicates were performed for each treatment, with each replicate containing 5–10 ovaries of *Nilaparvata lugens*

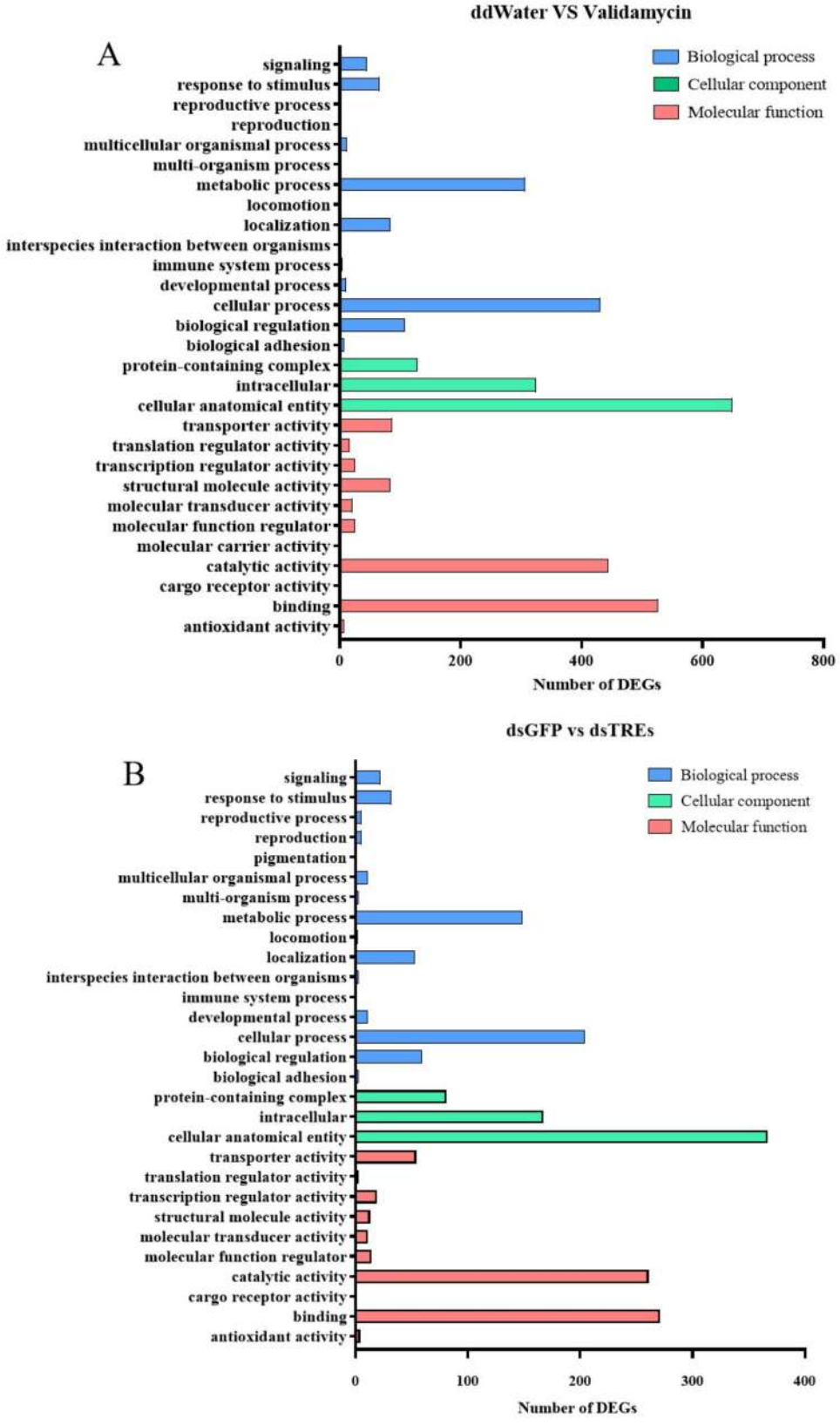

Fig. 2 GO functional classification of DEGs. (**A**) GO functional classification at level 2 of DEGs between the dsGFP and dsTREs groups; (**B**) GO functional classification at level 2 of DEGs between the ddWater and dsTREs groups

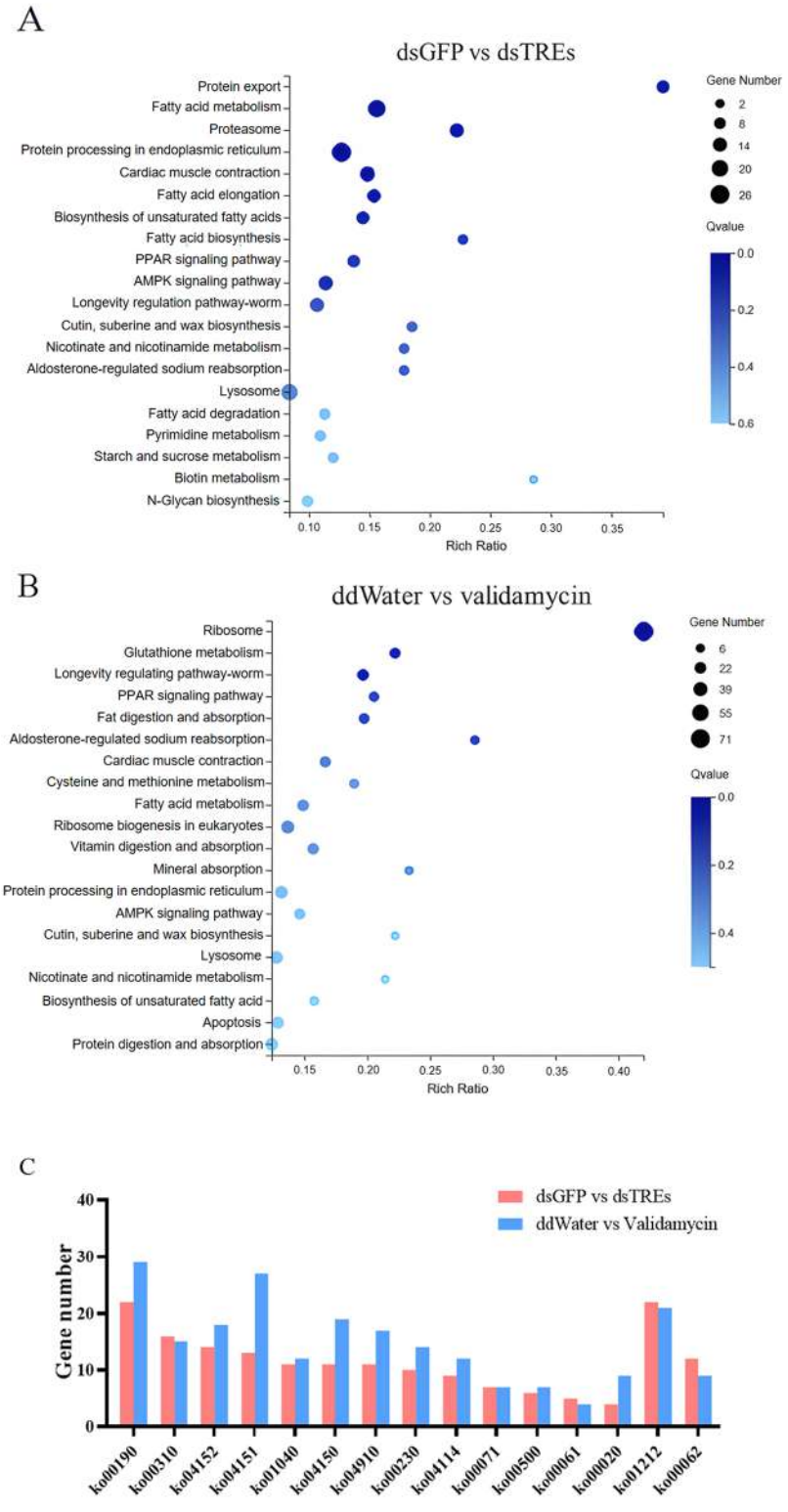

Fig. 3 KEGG metabolic pathway analysis of differentially expressed genes. (**A**) and (**B**) represent the top 20 metabolic pathways with the lowest q-values, (**C**) represents potential reproduction-related metabolic pathways. ko00190, oxidative phosphorylation; ko00310, Lysine degradation; ko04152, AMPK signaling pathway; ko04151, PI3K-Akt signaling pathway; ko01040, unsaturated fatty acid synthesis; ko04150, mTOR signaling pathway; ko04910, Insulin signaling pathway; ko00230, proline metabolism; ko04114, oocyte meiotic division; ko00071, fatty acid degradation; ko00500, starch and sucrose metabolism; ko00061, fatty acid synthesis; ko00020, TCA cycle; ko01212, fatty acid metabolism; ko00062, fatty acid elongation

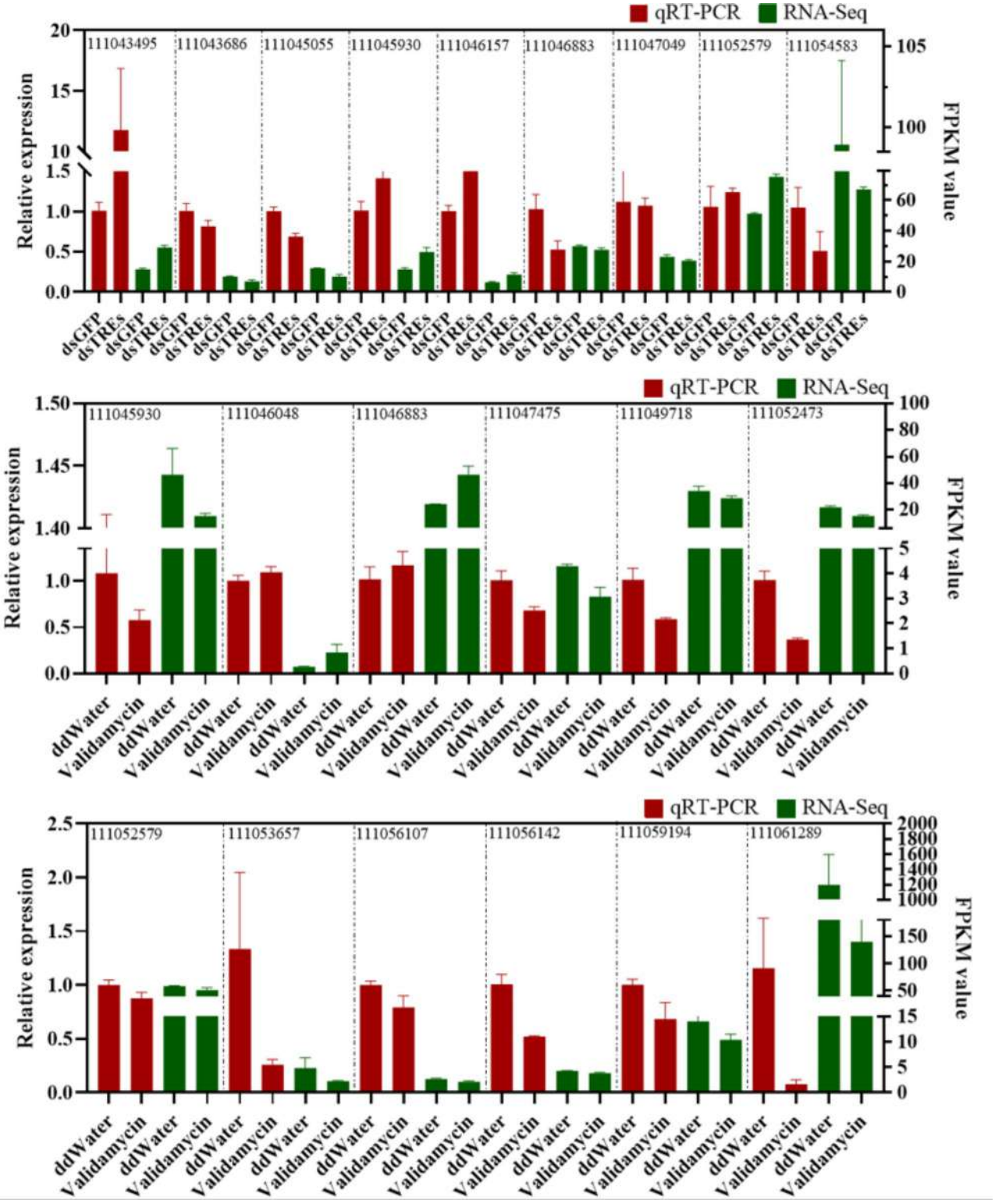

Fig. 4 RT-qPCR verification of DEGs. The data are shown as mean ± standard errors ($n = 3$). FPKM values represent the gene expression levels in the transcriptomics. Specific information about the selected genes is shown in Table 3

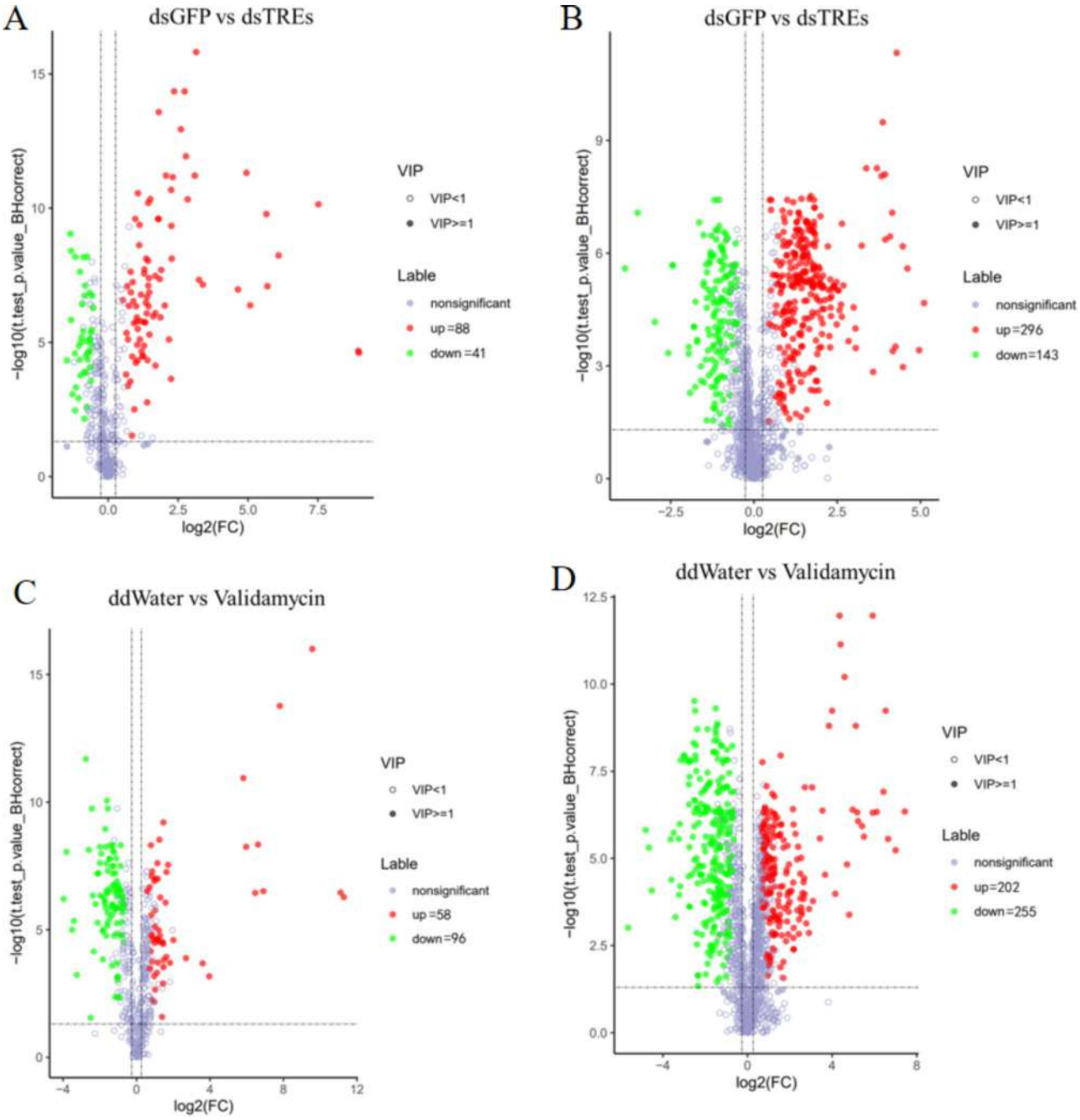

Fig. 5 Volcanic map of differential metabolites. (**A**) and (**C**) show the negative ion mode, while (**B**) and (**D**) show the positive ion mode

202 metabolites were up-regulated and 255 metabolites were down-regulated (Fig. 5D).

KEGG pathway enrichment and analysis of key metabolites

Results have shown that differential metabolites after dsTREs injection were mainly distributed in carbohydrate and amino acid-related metabolic pathways (Fig. 6A and B), while the differential metabolites between validamycin and water groups were also distributed in carbohydrate and amino acid-related metabolic pathways, but they were additionally significantly enriched in pyruvate metabolism, TCA cycle, oxidative phosphorylation, which were related to energy metabolism (Fig. 6C and D). In addition, the sucrose content was significantly increased in the ovaries of *N. lugens* treated with dsTREs or validamycin. Since sucrose is not present in insect ovary, and the molecular formula of sucrose is identical to that of trehalose, it is speculated that trehalose rather than sucrose is significantly accumulated in the ovaries after dsTREs or validamycin injection (Fig. 6E).

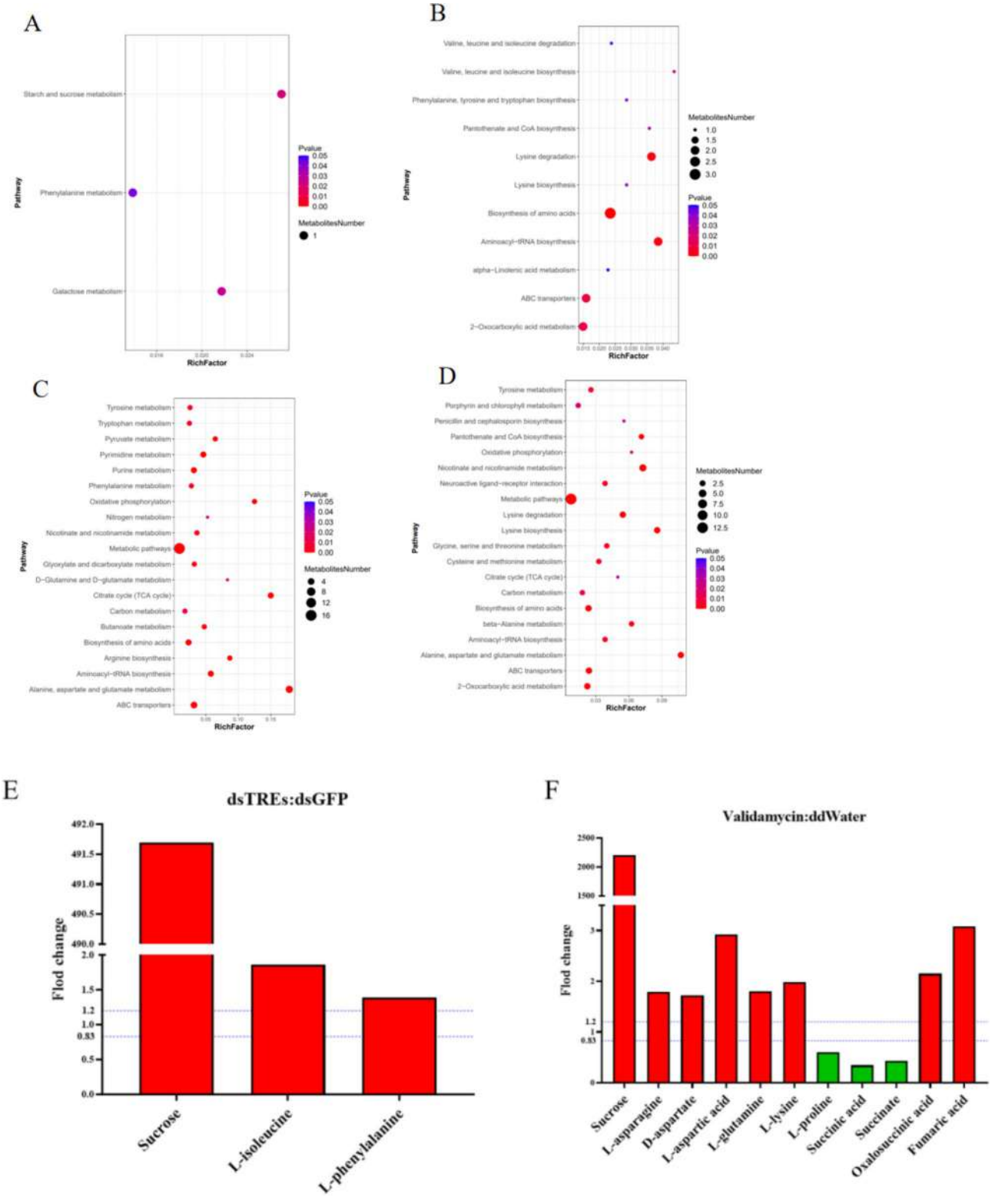

Fig. 6 KEGG pathway enrichment analysis of differential metabolites and analysis of crucial metabolites. The horizontal axis represents enrichment factors, and the vertical axis represents the top 20 enriched metabolic pathways. (**A**) and (**B**) represent the KEGG enrichment pathways between dsGFP and dsTREs groups in the negative ion and positive ion modes; (**C**) and (**D**) represent the KEGG enrichment pathway between ddWater and validamycin groups in the negative ion and positive ion mode. Red indicates up-regulated metabolites, and green indicates down-regulated metabolites in (**E**) and (**F**)

In addition, L-isoleucine and L-phenylalanine were significantly elevated in the ovaries after dsTREs injection (Fig. 6E). The levels of several amino acids in the ovaries were also up-regulated after validamycin injection, including L-asparagine, D-aspartic acid, L-aspartic acid, L-glutamine, and lysine, while the level of L-proline was significantly decreased (Fig. 6F). Unlike dsTREs, the intermediate metabolites involved in the TCA cycle in the ovaries of the validamycin group were also significantly affected. Among them, succinic acid and succinate were significantly down-regulated, whereas oxalosuccinic acid and fumaric acid were significantly up-regulated, indicating that the inhibition of trehalase by validamycin disrupts the TCA cycle in the ovaries of *N. lugens* (Fig. 6F).

Discussion

Trehalose hydrolyzed by TRE is involved in the synthesis of macromolecules such as chitin and lipids, indirectly affecting key signaling pathways that regulate the development and reproduction of the ovaries in insects [16, 24, 51, 54]. Chitin biosynthesis is a process in which trehalose acts as a precursor [24], undergoing a series of physiological and biochemical reactions that ultimately result in chitin synthesis by chitin synthase (CHS) [53]. Previous studies have shown that *TRE* silencing lead to an imbalance in the supply of trehalose, downregulating the expression of chitin synthase and decreasing chitin synthesis, which furthermore results in increased larval mortality and abnormalities [53, 66]. Chitin is also an important component of the egg chorion [55]. This study shows that the *TRE* inhibition leads to decreased expression of chitin synthesis-related genes (Fig. 3), suggesting that TRE deficiency may affect the composition of the egg chorion, ultimately influencing the hatchability of the offspring [55].

Furthermore, in oviparous insects, oocyte maturation requires not only the accumulation of Vg but also the accumulation of lipids [35, 56, 57]. The KEGG analysis show that DEGs in both the dsTREs and validamycin-treated groups are involved in metabolic pathways such as fatty acid synthesis, unsaturated fatty acid synthesis, and fatty acid elongation (Fig. 3). Previous studies have indicated that carbohydrates are essential for lipid synthesis, suggesting that TRE may reduce acetyl-CoA synthesis by affecting the tricarboxylic acid cycle and other glucose metabolism pathways, which in turn influences the production and utilization of mature fatty acids. Moreover, fatty acids are closely linked to reproduction in *N. lugens* [58]. Fatty acid metabolism is strongly associated with lipid synthesis. For example, studies in mice have shown that trehalose inhibits adipocyte hypertrophy [59]. Therefore, it is hypothesized that, *TRE* inhibition may disrupt lipid synthesis, which affected the ovarian development. Meanwhile, it was found that amino acids such as lysine and proline were also affected (Fig. 6). Previous studies have found that ovarian development and the number of eggs laid were affected after feeding on amino acid-deficient medium [63, 72]. Therefore, it is speculated that *TRE* knockdown inhibits the development of the ovaries in *N. lugens* by affecting the metabolism of amino acids and proteins in the ovaries. Besides, ribosomes serve as the sites of protein synthesis, and their synthesis and translation are blocked to suppress the ovarian development of insect [41], suggesting that validamycin also impacts protein synthesis to inhibit the reproduction of *N. lugens* [70, 71]. Accordingly, the DEGs in this group are extensively involved in metabolic pathways related to amino acids such as lysine and proline (Fig. 3). Moreover, previous study showed that the levels of lactic acid and alanine, which are involved in glycolysis, decreased within 0–12 h in the hemolymph of *Spodoptera litura* larvae treated with validamycin. These findings suggest that validamycin inhibits the glycolysis pathway [16]. This is consistent with this study, which partially have indicated that validamycin have affected glycolysis (Figs. 3 and 6).

TRE not only affects the energy substances such as carbohydrates, amino acids, and fatty acids, but also significantly alters the TCA cycle and oxidative phosphorylation that are responsible for energy production (Fig. 6). In insects, carbohydrates such as trehalose or glycogen are hydrolyzed into glucose, which then enters glycolysis and the TCA cycle. The resulting reduced NADH is further oxidized via oxidative phosphorylation to produce ATP for various cellular activities. Therefore, it is speculated that TRE have affected the energy production [64, 65, 67]. Reproduction is an energy-dependent process, and energy metabolism is closely related to ovarian development [68]. This suggests that validamycin may inhibit the TRE activity, which have resulted in insufficient ATP for cellular metabolism in the ovaries [52, 69].

Furthermore, transcriptome analysis revealed that the AMPK signaling pathway was altered after TRE inhibition, and AMPK modulated the mTOR and IIS signaling pathways [76, 77]. Notably, AMPK, as an energy sensor, is associated with carbohydrate metabolism and plays a regulatory role in insect oogenesis. Under normal energy conditions, AMPK pathway activity remains low, while the mTOR and IIS pathways are highly active [73, 74]. Activated mTOR phosphorylates S6K, which promotes the transcription and translation of Vg. In addition, mTOR stimulates the secretion of ILPs, thus activating the IIS pathway and inhibits the expression of genes such as FoxO, which suppresses the transcription and translation of Vg [75, 76]. When energy supply is insufficient or glucose starvation occurs, AMPK is activated. Activated AMPK activates TSC2 to inhibit mTOR, while also

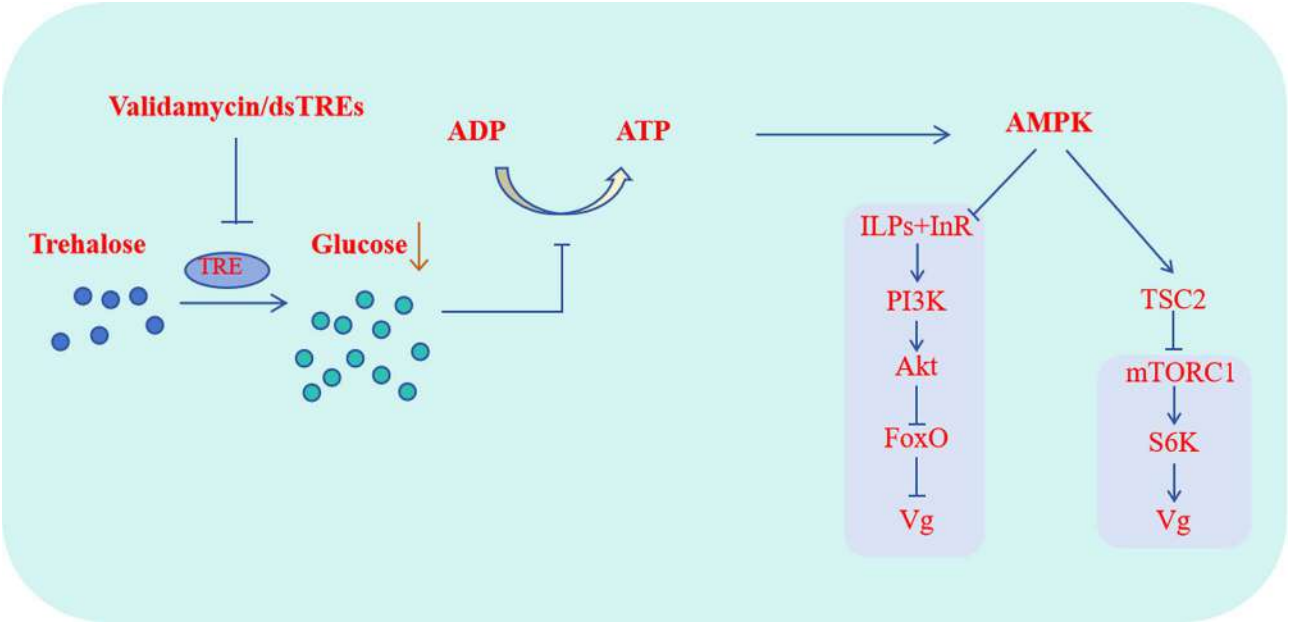

Fig. 7 The trehalase in *N. lugens* influences the regulatory network of reproduction. "→" represents a positive effect, and "⊥" represents a negative effect. ILP, insulin-like peptide; PI3K, phosphoinositide 3-kinase; Akt, protein kinase B; Foxo, forkhead box O; Vg, vitellogenin; TSC2, tuberous sclerosis complex 2; mTORC1, mechanistic target of rapamycin complex 1; S6K, S6 kinase

phosphorylating and inhibiting insulin-like pathway, ultimately affecting ovarian development and reproduction [78–80]. However, the number of DEGs in these signaling pathways was higher in the validamycin group compared to the dsTREs group, suggesting that the impact of validamycin on ovarian physiology is more extensive (Figs. 2 and 3).

In conclusion, it is speculated that TRE blocks ovarian energy production by affecting energy substances. However, the metabolomic analysis revealed no significant changes in glucose levels among the differential metabolites. Therefore, it is hypothesized that TRE does not affect the overall glucose level in the ovary, but may instead alter the intracellular glucose concentration gradient or the distribution of glucose among different ovarian cells. These changes could influence energy production, thus affecting the reproductive regulatory network and ultimately modulating reproduction in *N. lugens*.

Conclusions

The results showed that energy substance metabolism and the TCA cycle pathways were significantly enriched, indicating that *TRE* inhibition affects protein synthesis, fatty acid metabolism, and the energy cycle. These ultimately led to insufficient energy supply for ovarian development, reduced chitin content in the egg epidermis, and abnormal individual growth and development. Additionally, transcriptome analysis revealed that the AMPK signaling pathway was altered after *TRE* inhibition, and AMPK subsequently affected the mTOR and IIS signaling pathways. Furthermore, mTOR and IIS regulate Vg protein expression in *N. lugens*, thereby modulating reproduction in *N. lugens* (Fig. 7). In summary, our experimental results provide valuable insights for pest control in agriculture and the improvement of rice yield.

Abbreviations

TRE	Trehalase
N.lugens	*Nilaparvata lugens*
DEGs	Differentially expressed genes
AMPK	AMP-activated protein kinase
mTOR	Mammalian target of rapamycin
IIS	Insulin/Insulin-like growth factor signaling
TCA	The tricarboxylic acid
TRE1	Soluble trehalase
TRE2	Membrane-bound trehalase
TRE1-1	Trehalose-1-phosphate synthase 1–1
TRE1-2	Trehalose-1-phosphate receptor 1–2
ILPs	Initiated by insulin-like peptides
InR	Insulin receptor
PI3K	Phosphoinositide 3-kinase
PIP2	Phosphatidylinositol 4,5-diphosphate
PIP3	Phosphatidylinositol 3,4,5-trisphosphate
Akt	Protein Kinase B
FoxO	Forkhead box O
Vg	Vitellogenin
TOR	Target of rapamycin
TORC1	Target of rapamycin complex 1
TORC2	Target of rapamycin complex 2
AAs	Amino acids
S6K	Phosphorylation of S6 kinase
4E-BP1	4E-binding protein 1
RNA-seq	RNA sequencing
TN1	Taichung Native 1
dsRNA	Double-strand RNA
GFP	Green fluorescent protein
RT-qPCR	Reverse transcription quantitative polymerase chain reaction

LC-MS/MS	Liquid Chromatography-tandem mass spectrometry
PCA	Principal component analysis
VIP	Variable importance for the projection
PLS-DA	Partial least squares discriminant analysis
FC	Fold change
FDR	False discovery rate
RNAi	RNA interference
MF	Molecular function
CC	Cellular component
BP	Biological process
CHS	Chitin synthase
NADH	Nicotinamide adenine dinucleotide
TSC2	Tuberous sclerosis complex 2

Supplementary Information

The online version contains supplementary material available at https://doi.org/10.1186/s12864-025-11268-8.

Supplementary Material 1: **Figure S1**: The relative expression of *TRE1-1*, *TRE1-2* and *TRE2* after dsTREs injection. The data was shown as mean + standard errors ($n \geq 3$) and analyzed using Student's ***t*** test. "**", $P < 0.01$. **Figure S2**: GO functional classification of differential expression genes (DEGs). (A), GO functional classification of differential expression genes (DEGs); (B), GO functional classification in level 1 of DEGs between ddWater and validamycin groups.

Acknowledgements
Not Applicable.

Author contributions
Conceptualization, Y.K.L., X.L.T. and B.T.; methodology, L.Y. and S.J.W.; validation, X.Z.W. and L.W.G.; formal analysis, F.Y.; writing—original draft preparation, Y.K.L. and F.Y.; visualization, C.D.X. and B.H.X. All authors have read and agreed to the published version of the manuscript.

Funding
This research was supported by the National Natural Science Foundation of China (Grant No.32272608 and 32172415), the National Key R & D Program of China (grant numbers 2023YFE0104800) and by the ADOPT- IPM project funded by the European Union's Horizon Europe framework program (grant agreement number 101060430).

Data availability
Sequence data that support the findings of this study have been deposited in the National Center of Biotechnology Information with the primary accession code PRJNA1127067.

Declarations

Ethics approval and consent to participate
This is an analytical study. The Research Ethics Committee of Hangzhou Normal University has confirmed that ethical approval is not required.

Consent for publication
Not Applicable.

Competing interests
The authors declare no competing interests.

Received: 4 July 2024 / Accepted: 21 January 2025
Published online: 01 February 2025

References

1. Li L, Jiang Y, Liu Z, You L, Wu Y, Xu B, Ge L, Stanley D, Song Q, Wu J. Jinggangmycin increases fecundity of the brown planthopper, *Nilaparvata lugens* (Stål) via fatty acid synthase gene expression. J Proteom. 2016;130:140–9. https://doi.org/10.1016/j.jprot.2015.09.022.
2. Khush GS. What it will take to feed 5.0 billion rice consumers in 2030. Plant Mol Biol. 2005;59(1):1–6. https://doi.org/10.1007/s11103-005-2159-5.
3. Tuyen le Q, Liu Y, Jiang L, Wang B, Wang Q, Hanh TT, Wan J. Identification of quantitative trait loci associated with small brown planthopper (*Laodelphax striatellus* Fallén) resistance in rice (Oryza sativa L). Hereditas. 2012;149(1):16–23. https://doi.org/10.1111/j.1601-5223.2011.02231.x.
4. Lu K, Chen X, Liu W, Zhang Z, Wang Y, You K, Li Y, Zhang R, Zhou Q. Characterization of heat shock protein 70 transcript from *Nilaparvata lugens* (Stål): its response to temperature and insecticide stresses. Pestic Biochem Physiol. 2017;142:102–10. https://doi.org/10.1016/j.pestbp.2017.01.011.
5. Vijayakumar MM, More P, Rangasamy R, Gandhi AR, Muthugounder G, Thiruvengadam M, Samaddar V, K Jalali S, Sa S. Gut bacterial diversity of insecticide-susceptible and -resistant nymphs of the Brown Planthopper *Nilaparvata lugens* Stål (Hemiptera: Delphacidae) and elucidation of their putative functional roles. J Microbiol Biotechnol. 2018;28(6):976–86. https://doi.org/10.4014/jmb.1711.11039.
6. He J, Liu Y, Yuan D, Duan M, Liu Y, Shen Z, Yang C, Qiu Z, Liu D, Wen P, Huang J, Fan D, Xiao S, Xin Y, Chen X, Jiang L, Wang H, Yuan L, Wan J. An R2R3 MYB transcription factor confers brown planthopper resistance by regulating the phenylalanine ammonia-lyase pathway in rice. Proc Natl Acad Sci U S A. 2020;117(1):271–7. https://doi.org/10.1073/pnas.1902771116.
7. Qin Y, Xu P, Jin R, Li Z, Ma K, Wan H, Li J. Resistance of *Nilaparvata lugens* (Hemiptera: Delphacidae) to triflumezopyrim: inheritance and fitness costs. Pest Manag Sci. 2021;77(12):5566–75. https://doi.org/10.1002/ps.6598.
8. Wang Q, Fang K, Qi L, Wang X, Pan Y, Li Y, Xi J, Zhang J. Purification and functional characterization of a Soluble Trehalase in *Lissorhoptrus oryzophilus* (Coleoptera: Curculionidae). Insects. 2022;13(10):867. https://doi.org/10.3390/insects13100867.
9. Kim DS, Zhang J. Strategies to improve the efficiency of RNAi-mediated crop protection for pest control. Entomol Generalis. 2023;43(1):5–19. https://doi.org/10.1127/entomologia/2022/1638.
10. Su S, Zuo YY, Zhang XH, Jian CZ, Peng X, Piñero JC, Chen MH. Efficient CRISPR/Cas9-mediated white gene editing in the global tortricid fruit pest *Grapholita molesta*. Entomol Generalis. 2022;42(2):987–96. https://doi.org/10.1127/entomologia/2022/1563.
11. Wei D, Wang S, Niu JZ. RNAi-based pesticides: current knowledge and potential applications for Integrated Pest Management. Entomol Generalis. 2023;43(1):1–4. https://doi.org/10.1127/entomologia/2023/1988.
12. Lu J, Shen J. Target genes for RNAi in pest control: a comprehensive overview. Entomol Generalis. 2024;44(1):95–114. https://doi.org/10.1127/entomologia/2023/2207.
13. Jin LQ, Xue YP, Zheng YG, Shen YC. Production of trehalase inhibitor validoxylamine A using acid-catalyzed hydrolysis of validamycin A. Catal Commun. 2006;7(3):157–61. https://doi.org/10.1016/j.catcom.2005.10.004.
14. Veliz EA, Martínez-Hidalgo P, Hirsch AM. Chitinase-producing bacteria and their role in biocontrol. AIMS Microbiol. 2017;3(3):689–705. https://doi.org/10.3934/microbiol.2017.3.689.
15. Elbein AD, Pan YT, Pastuszak I, Carroll D. New insights on trehalose: a multifunctional molecule. Glycobiology. 2003;13(4):17. https://doi.org/10.1093/glycob/cwg047. R-27R.
16. Shukla E, Thorat LJ, Nath BB, Gaikwad SM. Insect trehalase: physiological significance and potential applications. Glycobiology. 2015;25(4):357–67. https://doi.org/10.1093/glycob/cwu125.
17. Liebl M, Nelius V, Kamp G, Ando O, Wegener G. Fate and effects of the trehalase inhibitor trehazolin in the migratory Locust (Locusta migratoria). J Insect Physiol. 2010;56(6):567–74. https://doi.org/10.1016/j.jinsphys.2009.11.021.
18. Wu Z, Gao J, Wang X, Wang C, Zhang C, Li X, Zhang J, Sun Y. Soluble trehalase responds to heavy metal stimulation by regulating apoptosis in Neocaridina denticulata sinensis. Ecotoxicol Environ Saf. 2024;285:117072. https://doi.org/10.1016/j.ecoenv.2024.117072.
19. Chen J, Tang B, Chen H, Yao Q, Huang X, Chen J, Zhang D, Zhang W. Different functions of the insect soluble and membrane-bound trehalase genes in chitin biosynthesis revealed by RNA interference. PLoS ONE. 2010;5(4):e10133. https://doi.org/10.1371/journal.pone.0010133.
20. Tang B, Qin Z, Shi ZK. Trehalase in Harmonia axyridis (Coleoptera: Coccinellidae): effects on beetle locomotory activity and the correlation with trehalose metabolism under starvation conditions. Appl Entomol Zool. 2014;49:255–64. https://doi.org/10.1007/s13355-014-0244-4.
21. Wang Z, Long GY, Jin DC, Yang H, Zhou C, Yang XB. Knockdown of two trehalase genes by RNA interference is Lethal to the White-Backed Planthopper

Sogatella furcifera (Horváth) (Hemiptera: Delphacidae). Biomolecules. 2022;12(11):1699. https://doi.org/10.3390/biom12111699.
22. Wu Q, Brown MR. Signaling and function of insulin-like peptides in insects. Annu Rev Entomol. 2006;51:1–24. https://doi.org/10.1146/annurev.ento.51.110104.151011.
23. García MD, Argüelles JC. Trehalase inhibition by validamycin A may be a promising target to design new fungicides and insecticides. Pest Manag Sci. 2021;77(9):3832–5. https://doi.org/10.1002/ps.6382.
24. Tang B, Wei P, Zhao L, Shi Z, Shen Q, Yang M, Xie G, Wang S. Knockdown of five trehalase genes using RNA interference regulates the gene expression of the chitin biosynthesis pathway in *Tribolium castaneum*. BMC Biotechnol. 2016;16(1):67. https://doi.org/10.1186/s12896-016-0297-2.
25. Li Y, Wang SS, Si HR, Wan SJ, Li GY, Shu YH, Dai XY, Wang RJ, Wang SG, Zhai YF, Li C, Tang B. Responses of aphid and ladybird to lead transfer through soil and broad beans. Entomol Generalis. 2024. https://doi.org/10.1127/entomologia/2023/2277.
26. Liu Y-K, Luo Y-J, Deng Y-M, Li Y, Pang X-Q, Xu C-D, Wang S-G. Bin Tang. Insulin receptors regulate the fecundity of *Nilaparvata lugens* (Stål) (Hemiptera: Delphacidae),Journal of Asia-Pacific Entomology. 2020;23(4):1151–9. https://doi.org/10.1016/j.aspen.2020.09.011
27. Dong Y, Chen W, Kang K, Pang R, Dong Y, Liu K, Zhang W. FoxO directly regulates the expression of TOR/S6K and vitellogenin to modulate the fecundity of the brown planthopper. Sci China Life Sci. 2021;64(1):133–43. https://doi.org/10.1007/s11427-019-1734-6.
28. Wullschleger S, Loewith R, Hall MN. TOR signaling in growth and metabolism. Cell. 2006;124(3):471–84. https://doi.org/10.1016/j.cell.2006.01.016.
29. Smykal V, Raikhel AS. Nutritional Control of Insect Reproduction. Curr Opin Insect Sci. 2015;11:31–8. https://doi.org/10.1016/j.cois.2015.08.003.
30. Tang B, Hu S, Luo Y, Shi D, Liu X, Zhong F, Jiang X, Hu G, Li C, Duan H, Wu Y. Impact of three Thiazolidinone compounds with Piperine skeletons on Trehalase Activity and Development of *Spodoptera frugiperda* Larvae. J Agric Food Chem. 2024;72(15):8423–33. https://doi.org/10.1021/acs.jafc.3c08898.
31. Bai L, Li L, Xu H, Minagawa K, Yu Y, Zhang Y, Zhou X, Floss HG, Mahmud T, Deng Z. Functional analysis of the validamycin biosynthetic gene cluster and engineered production of validoxylamine A. Chem Biol. 2006;13(4):387–97. https://doi.org/10.1016/j.chembiol.2006.02.002.
32. Matassini C, Parmeggiani C, Cardona F. New Frontiers on Human Safe insecticides and fungicides: an opinion on Trehalase inhibitors. Molecules. 2020;25(13):3013. https://doi.org/10.3390/molecules25133013.
33. Thuy BTP, My TTA, Hai NTT. A molecular docking simulation study on potent inhibitors against *Rhizoctonia solani* and *Magnaporthe oryzae* in rice: silver-tetrylene and bis-silver-tetrylene complexes vs. validamycin and tricyclazole pesticides. Struct Chem Struct Chem. 2021;32:135–48. https://doi.org/10.1007/s11224-020-01627-4.
34. Katewa SD, Kapahi P. Role of TOR signaling in aging and related biological processes in *Drosophila melanogaster*. Exp Gerontol. 2011;46(5):382–90. https://doi.org/10.1016/j.exger.2010.11.036.
35. Komatsu K, Masubuchi S. Observation of the dynamics of follicular development in the ovary. Reprod Med Biol. 2016;16(1):21–7. https://doi.org/10.1002/rmb2.12010.
36. Jarrett BY, Vanden Brink H, Brooks ED, Hoeger KM, Spandorfer SD, Pierson RA, Chizen DR, Lujan ME. Impact of right-left differences in ovarian morphology on the ultrasound diagnosis of polycystic ovary syndrome. Fertil Steril. 2019;112(5):939–46. https://doi.org/10.1016/j.fertnstert.2019.06.016.
37. Luo S, Li J, Liu X, Lu Z, Pan W, Zhang Q, Zhao Z. Effects of six sugars on the longevity, fecundity and nutrient reserves of *Microplitis mediator*. Biol Control. 2010;52(1):51–7. https://doi.org/10.1016/j.biocontrol.2009.09.002.
38. Santos R, Alves-Bezerra M, Rosas-Oliveira R, Majerowicz D, Meyer-Fernandes JR, Gondim KC. Gene identification and enzymatic properties of a membrane-bound trehalase from the ovary of *Rhodnius prolixus*. Arch Insect Biochem Physiol. 2012;81(4):199–213. https://doi.org/10.1002/arch.21043.
39. Olivier M, Asmis R, Hawkins GA, Howard TD, Cox LA. The need for Multi-omics Biomarker signatures in Precision Medicine. Int J Mol Sci. 2019;20(19):4781. https://doi.org/10.3390/ijms20194781.
40. Jing S, Zhao Y, Du B, Chen R, Zhu L, He G. Genomics of interaction between the brown planthopper and rice. Curr Opin Insect Sci. 2017;19:82–7. https://doi.org/10.1016/j.cois.2017.03.005.
41. Li Y, Wang SS, Wang S, Wang SG, Tang B, Liu F. Involvement of glucose transporter 4 in ovarian development and reproductive maturation of *Harmonia axyridis* (Coleoptera: Coccinellidae). Insect Sci. 2021;29(3):691–703. https://doi.org/10.1111/1744-7917.12972.
42. Liu C, Yang L, Jin F, Yin Y, Xie Z, Yang L, Zhao S, Zhang G, Yang D, Han X. Untargeted UHPLC-MS Metabolomics reveals the metabolic perturbations of *Helicoverpa armigera* under the stress of Novel Insect Growth Regulator ZQ-8. Agronomy. 2023;13(5):1315. https://doi.org/10.3390/agronomy13051315.
43. Wang LL, Smagghe G, Swevers L, Lu YY. Metabolomics-based approaches in unraveling virus infections in insects: revealing unknown hidden interactions. Entomol Generalis. 2024. https://doi.org/10.1127/entomologia/2024/2213. n. pag.
44. Hrdlickova R, Toloue M, Tian B. RNA-Seq methods for transcriptome analysis. Wiley Interdiscip Rev RNA. 2017;8(1). https://doi.org/10.1002/wrna.1364.
45. Wang Z, Gerstein M, Snyder M. RNA-Seq: a revolutionary tool for transcriptomics. Nat Rev Genet. 2009;10(1):57–63. https://doi.org/10.1038/nrg2484.
46. Stark R, Grzelak M, Hadfield J. RNA sequencing: the teenage years. Nat Rev Genet. 2019;20(11):631–56. https://doi.org/10.1038/s41576-019-0150-2.
47. Katam R, Lin C, Grant K, Katam CS, Chen S. Advances in Plant Metabolomics and its applications in stress and single-cell Biology. Int J Mol Sci. 2022;23(13):6985. https://doi.org/10.3390/ijms23136985.
48. Schrimpe-Rutledge AC, Codreanu SG, Sherrod SD, McLean JA. Untargeted Metabolomics Strategies-challenges and emerging directions. J Am Soc Mass Spectrom. 2016;27(12):1897–905. https://doi.org/10.1007/s13361-016-1469-y.
49. Zhao J, Xie C, Wang K, Takahashi S, Krausz KW, Lu D, Wang Q, Luo Y, Gong X, Mu X, Wang Q, Su S, Gonzalez FJ. Comprehensive analysis of transcriptomics and metabolomics to understand triptolide-induced liver injury in mice. Toxicol Lett. 2020;333:290–302. https://doi.org/10.1016/j.toxlet.2020.08.007.
50. Cheng J, Pan Y, Yang S, Wei Y, Lv Q, Xing Q, Zhang R, Sun L, Qin G, Shi D, Deng Y. Integration of transcriptomics and non-targeted metabolomics reveals the underlying mechanism of follicular atresia in Chinese buffalo. J Steroid Biochem Mol Biol. 2021;212:105944. https://doi.org/10.1016/j.jsbmb.2021.105944.
51. Chen JX, Lyu ZH, Wang CY, Cheng J, Lin T. RNA interference of a trehalose-6-phosphate synthase gene reveals its roles in the biosynthesis of chitin and lipids in *Heortia vitessoides* (Lepidoptera: Crambidae). Insect Sci. 2020;27(2):212–23. https://doi.org/10.1111/1744-7917.12650.
52. Tang Bin W, Ping C, Jie WS-G. Zhang Wen-Qing. Progress in gene features and functions of insect trehalases. Acta Entomologica Sinica. 2012;55(11):1315–21. https://doi.org/10.16380/j.kcxb.2012.55.11.13151321.
53. Zhao L, Yang M, Shen Q, Liu X, Shi Z, Wang S, Tang B. Functional characterization of three trehalase genes regulating the chitin metabolism pathway in rice brown planthopper using RNA interference. Sci Rep. 2016;6:27841. https://doi.org/10.1038/srep27841.
54. Tang B, Yang M, Shen Q, Xu Y, Wang H, Wang S. Suppressing the activity of trehalase with validamycin disrupts the trehalose and chitin biosynthesis pathways in the rice brown planthopper, *Nilaparvata lugens*. Pestic Biochem Physiol. 2017;137:81–90. https://doi.org/10.1016/j.pestbp.2016.10.003.
55. Masuda H, Melo AC, Moreira MF. Effects of chitin synthase double-stranded RNA on molting and oogenesis in the Chagas disease vector Rhodnius prolixus. Insect Biochem Mol Biol. 2014. https://doi.org/10.1016/j.ibmb.2013.12.006. 51110-121.
56. Athenstaedt K, Daum G. The life cycle of neutral lipids: synthesis, storage and degradation. Cell Mol Life Sci. 2006;63(12):1355–69. https://doi.org/10.1007/s00018-006-6016-8.
57. Arrese EL, Soulages JL. Insect fat body: energy, metabolism, and regulation. Annu Rev Entomol. 2010;55:207–25. https://doi.org/10.1146/annurev-ento-112408-085356.
58. Vrablik TL, Watts JL. Polyunsaturated fatty acid derived signaling in reproduction and development: insights from Caenorhabditis elegans and *Drosophila melanogaster*. Mol Reprod Dev. 2013;80(4):244–59. https://doi.org/10.1002/mrd.22167.
59. Arai C, Suyama A, Arai S, Arai N, Yoshizane C, Koya-Miyata S, Mizote A, Endo S, Ariyasu T, Mitsuzumi H, Ushio S. Trehalose itself plays a critical role on lipid metabolism: Trehalose increases Jejunum cytoplasmic lipid droplets which negatively correlated with mesenteric adipocyte size in both HFD-fed trehalase KO and WT mice. Nutr Metab (Lond). 2020;17:22. https://doi.org/10.1186/s12986-020-00443-1.
60. Kim D, Langmead B, Salzberg SL. HISAT: a fast spliced aligner with low memory requirements. Nat Methods. 2015;12(4):357–60. https://doi.org/10.1038/nmeth.3317.
61. Langmead B, Salzberg SL. Fast gapped-read alignment with Bowtie 2. Nat Methods. 2012;9(4):357–9. https://doi.org/10.1038/nmeth.1923.
62. Anders S, Huber W. Differential expression analysis for sequence count data. Genome Biol. 2010;11(10):R106. https://doi.org/10.1186/gb-2010-11-10-r106.

63. Pan X, Lu K, Qi S, Zhou Q, Zhou Q. The content of amino acids in artificial diet influences the development and reproduction of brown planthopper, *Nilaparvata lugens* (STÅL). Arch Insect Biochem Physiol. 2014;86(2):75–84. https://doi.org/10.1002/arch.21162.
64. Sisodia S, Singh BN. Experimental evidence for nutrition regulated stress resistance in *Drosophila ananassae*. PLoS ONE. 2012;7(10):e46131. https://doi.org/10.1371/journal.pone.0046131.
65. Dewar CE, Casas-Sanchez A, Dieme C, Crouzols A, Haines LR, Acosta-Serrano Á, Rotureau B, Schnaufer A. Oxidative phosphorylation is required for powering motility and development of the sleeping sickness parasite trypanosoma brucei in the tsetse fly Vector. mBio. 2022;13(1):e0235721. https://doi.org/10.1128/mbio.02357-21.
66. Peng Z, Green PG, Arakane Y, Kanost MR, Gorman MJ. A multicopper oxidase-related protein is essential for insect viability, longevity and ovary development. PLoS ONE. 2014;9(10):e111344. https://doi.org/10.1371/journal.pone.0111344.
67. Mills E, O'Neill LA. Succinate: a metabolic signal in inflammation. Trends Cell Biol. 2014;24(5):313–20. https://doi.org/10.1016/j.tcb.2013.11.008.
68. Lorenz MW, Gäde G. Hormonal regulation of energy metabolism in insects as a driving force for performance. Integr Comp Biol. 2009;49(4):380–92. https://doi.org/10.1093/icb/icp019.
69. Shi S, Zuo H, Gao L, Yi X, Zhong G. Silencing of Rieske Iron-Sulfur protein impacts upon the Development and Reproduction of *Spodoptera exigua* by regulating ATP synthesis. Front Physiol. 2018;9:575. https://doi.org/10.3389/fphys.2018.00575.
70. Suzuki T, Sakurai S, Iwami M. Rectal sac distention is induced by 20-hydroxyecdysone in the pupa of *Bombyx mori*. J Insect Physiol. 2009;55(3):250–4. https://doi.org/10.1016/j.jinsphys.2008.11.014.
71. Sun Z, Shi JH, Fan T, Wang C, Liu L, Jin H, Foba CN, Wang MQ. The control of the brown planthopper by the rice Bph14 gene is affected by nitrogen. Pest Manag Sci. 2020;76(11):3649–56. https://doi.org/10.1002/ps.5911.
72. Wang W, Yang RR, Peng LY, Zhang L, Yao YL, Bao YY. Proteolytic activity of the proteasome is required for female insect reproduction. Open Biol. 2021;11(2):200251. https://doi.org/10.1098/rsob.200251.
73. Mihaylova MM, Shaw RJ. The AMPK signalling pathway coordinates cell growth, autophagy and metabolism. Nat Cell Biol. 2011;13(9):1016–23. https://doi.org/10.1038/ncb2329.
74. Herzig S, Shaw RJ. AMPK: guardian of metabolism and mitochondrial homeostasis. Nat Rev Mol Cell Biol. 2018;19(2):121–35. https://doi.org/10.1038/nrm.2017.95.
75. Hardie DG. AMP-activated protein kinase: an energy sensor that regulates all aspects of cell function. Genes Dev. 2011;25(18):1895–908. https://doi.org/10.1101/gad.17420111.
76. Shaw RJ. LKB1 and AMP-activated protein kinase control of mTOR signalling and growth. Acta Physiol (Oxf). 2009;196(1):65–80. https://doi.org/10.1111/j.1748-1716.2009.01972.x.
77. Yuan D, Zhou S, Liu S, Li K, Zhao H, Long S, Liu H, Xie Y, Su Y, Yu F, Li S. The AMPK-PP2A axis in insect fat body is activated by 20-hydroxyecdysone to antagonize insulin/IGF signaling and restrict growth rate. Proc Natl Acad Sci U S A. 2020;117(17):9292–301. https://doi.org/10.1073/pnas.2000963117.
78. Gautam S, Ishrat N, Yadav P, Singh R, Narender T, Srivastava AK. 4-Hydroxyisoleucine attenuates the inflammation-mediated insulin resistance by the activation of AMPK and suppression of SOCS-3 coimmunoprecipitation with both the IR-β subunit as well as IRS-1. Mol Cell Biochem. 2016;414(1–2):95–104. https://doi.org/10.1007/s11010-016-2662-9.
79. Oringanje C, Delacruz LR, Han Y, Luckhart S, Riehle MA. Overexpression of activated AMPK in the *Anopheles stephensi* midgut impacts Mosquito Metabolism, Reproduction and *Plasmodium* Resistance. Genes (Basel). 2021;12(1):119. https://doi.org/10.3390/genes12010119.
80. Jiang H, Zhang N, Ji C, Meng X, Qian K, Zheng Y, Wang J. Metabolic and transcriptome responses of RNAi-mediated AMPKα knockdown in *Tribolium castaneum*. BMC Genomics. 2020;21(1):655. https://doi.org/10.1186/s12864-020-07070-3.

Publisher's note